Reset Circuits With Energy Recovery for Solid-State Modulators

Juergen Biela, *Member, IEEE*, Dominik Bortis, *Student Member, IEEE*, and Johann W. Kolar, *Senior Member, IEEE*

Abstract—In power modulators for pulses in the microsecond range, transformers are often used for generating high output voltages. With standard topologies, the transformer is usually only excited in a unipolar direction, i.e., the flux density B swings between zero and a value close to the saturation flux density. By applying a reset circuit, the flux density B in the transformer is set to a value close to the negative saturation flux density before the pulse, so that the flux density could swing between the negative and positive saturation values during the pulse. This allows one to halve the core area and reduce the core volume/weight as well as the losses. In this paper, the operating modes of three different reset circuit topologies (the standard and a new advanced passive as well as an active one) and the corresponding waveforms are explained. Furthermore, the three topologies are compared with respect to the losses/complexity based on a design for a solid-state modulator with 20-MW output power and 200-kV output voltage.

Index Terms—Energy recovery, premagnetization, pulse transformer, reset circuit, solid-state modulator.

I. INTRODUCTION

PULSED POWER systems are used in a wide variety of applications, for example, in particle accelerators, radars, medical radiation, sterilization systems (e.g., drinking water), or ion implantation systems (semiconductor manufacturing). In these applications, pulses of several kilovolts and megawatts are generated, and the duration of the single pulse varies from a few nanoseconds to some milliseconds. The requirements on the generated pulses regarding, e.g., rise/fall time, overshoot, pulse flatness, and pulse energy are high and can vary over a wide range. Therefore, many different topologies are applied in pulsed power systems [1]–[3].

A lot of pulsed power systems (e.g., the one shown in Fig. 1) use a pulse transformer to step the output voltage up. The design of a pulse transformer is comparable to high-frequency (HF) transformers which are widely used in power electronics. However, in contrast to many converter topologies using HF transformers, pulse power systems only generate repeated unipolar voltage pulses. In this case, the core material of the pulse transformer is not optimally utilized.

The unipolar voltage pulse leads to a unipolar flux swing ΔB_1 in the core (cf. Fig. 2). This results in a core volume approximately twice as big as with a bipolar ΔB_2 excitation.
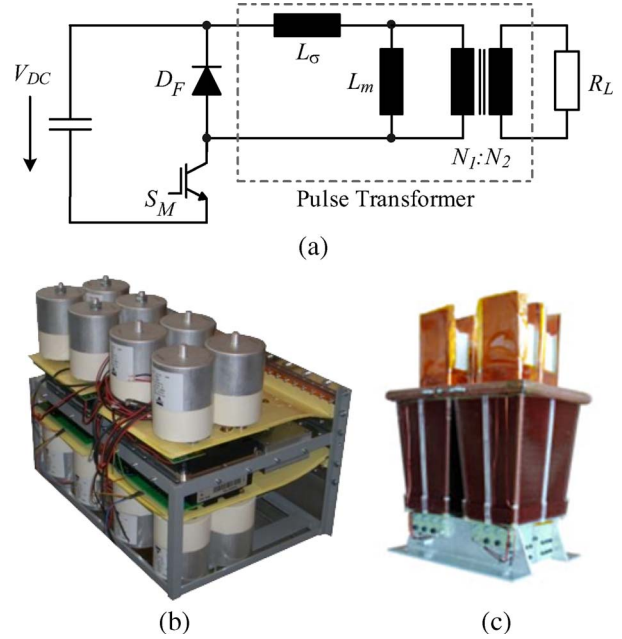
Fig. 1. (a) Schematic of a solid-state modulator with IGBTs and photo of the (b) modulator ($W \times L \times H = 45 \times 25 \times 35$ cm) as well as of the (c) transformer.
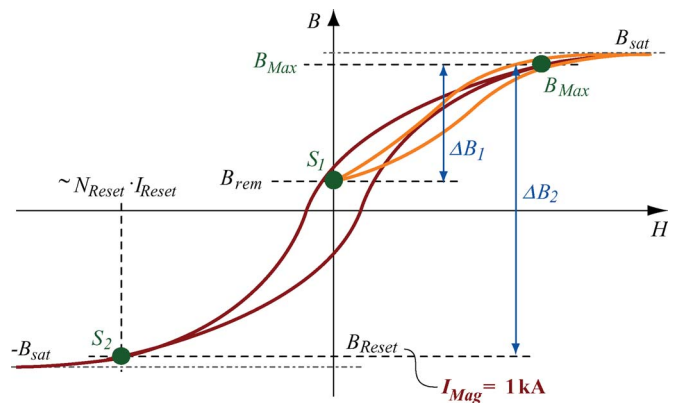

Fig. 2. Schematic magnetization curve with unipolar flux swing ΔB_1, bipolar flux swing $\Delta B_2 (\approx 2 \times \Delta B_1)$, and negative premagnetization B_{Reset}. This curve is derived from measured B–H loops of AMCC25 cores made of 2605SA1/Metglas.

A bipolar flux swing operation of the transformer could be achieved with a reset circuit which premagnetizes the core to a negative flux density B_{Reset} (S_2) before the pulse.

The most common method to reset transformer cores is the dc reset circuit (cf. Fig. 3), where a dc current is used to premagnetize the core [4]. The current flows in a direction that generates a magnetic flux (cf. B_{Reset} in Fig. 2) which is in the opposite
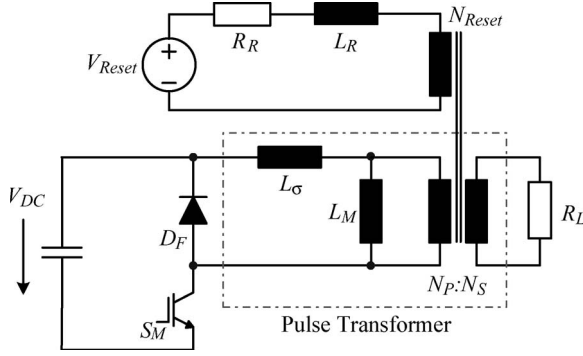
Fig. 3. Schematic of passive reset circuit.

TABLE I
SPECIFICATION OF THE CONSIDERED PULSE
MODULATOR WITH RESET CIRCUIT

DC link voltage	1000V	Output voltage	200kV
Output current	100A	Pulse Duration	$5\mu s$
Pulsed Output Power	20MW	Pulse Energy	100J
Repetition Rate	200Hz	Magnetizing Inductance	$2.5\mu H$
Magnetizing Current	1kA	Turns ratio	1:200

direction than the flux induced by the voltage pulse. Therefore, a flux swing ΔB_2 from a negative S_2 to a positive operation point B_{Max} instead of form zero (remanence S_1) to a positive operation point is possible. This increases the total possible peak-to-peak flux swing ΔB_2 by a factor of approximately two compared to a circuit without reset circuit and results in a significant reduction of the core cross section/volume and of the winding losses due to shorter turn lengths.

Basically, this current can be supplied to the primary, secondary, or tertiary windings. In order to keep the considerations more general, a tertiary winding, also called reset winding, is assumed in this paper.

During the operation, however, high losses (≈ 1.5 kW in the considered case) are generated since the energy stored in the magnetizing/leakage inductor and the energy stored during the pulse in the dc inductor are dissipated in the freewheeling diode D_F as explained in [4]. In order to recover part of the losses, a new dc reset circuit is presented in this paper [5], which is based on low-voltage technology common, e.g., in automotive converters. With this circuit, the energy stored in the premagnetizing inductor could be fed back to the reset circuit supply. This results in significantly lower losses compared to the standard passive reset circuit.

The energy stored in the magnetizing/leakage inductance, however, is still dissipated in the freewheeling diode. In order to also recover these losses, an active reset circuit is required [6]–[8]. There, the energy stored in the inductors is largely recovered to an additional capacitor and reused for premagnetizing the transformer before the next pulse. This leads to a further significant reduction of the losses due to the premagnetization and an improved efficiency.

In order to judge the losses and component effort of these three reset circuit topologies, the efficiency and component stresses are compared for the specifications given in Table I in this paper. Furthermore, the basic operation principle is explained, which has not been done before in detail.
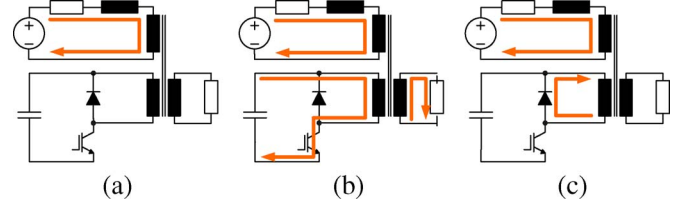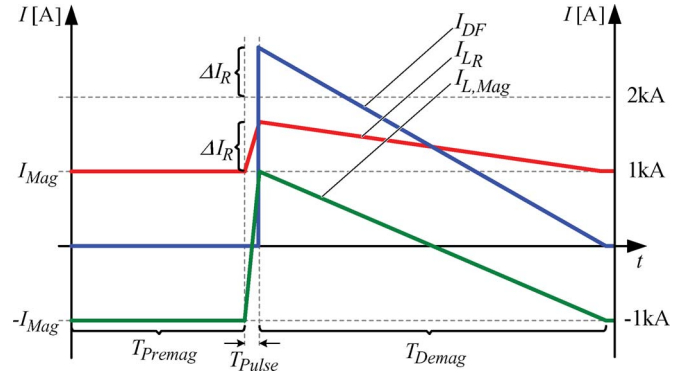

Fig. 4 Current paths for the passive reset circuit in the three time sections: premagnetization, pulse, and demagnetization. (a) Premagnetization. (b) Pulse. (c) Demagnetization.

Fig. 5 Run of the current I_{DF} in the freewheeling diode D_F, the magnetizing current $I_{L,\mathrm{Mag}}$, and the current I_{L_R} in the premagnetization inductance L_R.

First, the standard dc reset is described shortly in Section II. Then, the new improved passive reset circuit is explained in Section III, and the functionality of the active circuit is presented in Section IV. After the explanation of the three circuits, the comparison of the losses and component stress is given in Section V. Finally, a conclusion and topics of future research are presented in Section VI.

II. PASSIVE RESET CIRCUIT

In the following, the standard passive reset circuit shown in Fig. 3 is shortly explained (details can be found, e.g., in [4]). There and in the explanations of the advanced passive and active reset circuits, the influence of the leakage inductance is omitted since its influence on the efficiency is very small.

The circuit consists of a dc voltage V_{Reset} source, an inductor L_R with relatively large inductance (usually in the millihenry range), and the parasitic resistance R_R of the inductor/third winding. Due to the voltage source, a dc current flows through the inductor and the third winding, which premagnetizes the core negatively to B_{Reset} (cf. Figs. 2 and 4(a)). There, the amplitude of the current is determined by V_{Reset}/R_R.

As soon as the main switch S_M is closed, the dc link voltage V_{dc} is applied to the primary winding N_P, and the magnetic flux density starts to rise from B_{Reset} to B_{Max}, which results in a change of the magnetization current from $-I_{\mathrm{Mag}} = I_{\mathrm{Reset}}$ to I_{Mag} (cf. T_{Pulse} in Figs. 4(b) and 5). Furthermore, the primary voltage is not only reflected to the secondary but also to the tertiary winding. This leads to an increasing current I_{L_R}/stored energy in the reset inductor L_R

$$\Delta E_{L_R} = \frac{1}{2} L_R \left((I_{R,T} + \Delta I_{R,T})^2 - I_{R,T}^2 \right). \quad (1)$$

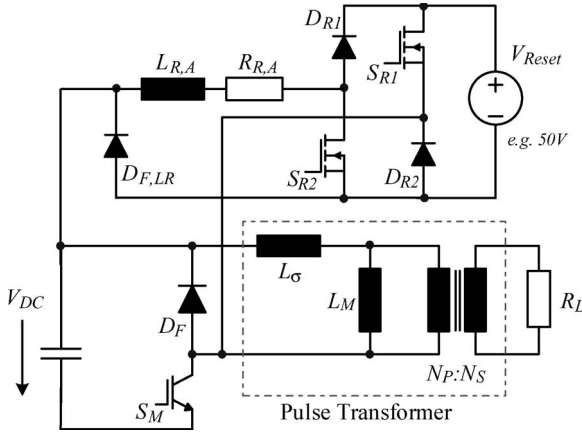There, $I_{R,T}$ is the reset current I_R on the tertiary side.

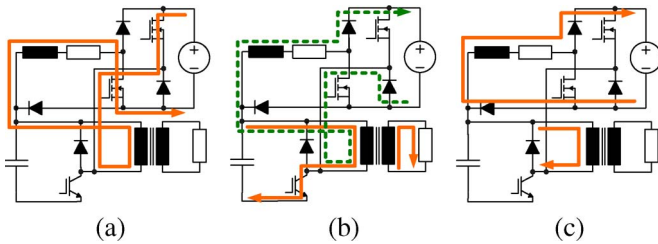Fig. 6. Proposed advanced passive reset circuit.

Fig. 7. Current paths for the advanced passive reset circuit in the three time sections: premagnetization, pulse, and demagnetization. (Interlocking time is omitted for the sake of brevity.) (a) Premagnetization. (b) Pulse. (c) Demagnetization.

After the pulse, the magnetization current flows via the freewheeling diode. Additionally, the current in L_R (reflected to the primary due to the negative di/dt) flows there, and the energy stored in the magnetizing inductance L_M as well as the additional energy stored in L_R due to the $\Delta I_{R,T}$ (cf. (1)) must be dissipated in the freewheeling diode until the initial state with constant premagnetization current is reached again.

With the considered specifications (cf. Table I), approximately 90% of this energy is provided by the pulse source (dc link capacitor) and 10% by the source V_{Reset} of the premagnetization. In order that the demagnetization ends before the next pulse, the forward voltage of the freewheeling diode D_F must not be too small. In the considered case, a forward voltage of approximately 10 V (a series connection of four diodes APT DF430U10G resulting in a demagnetization time of $T_{\text{Demag}} = 250$ μs) is assumed.

III. ADVANCED PASSIVE RESET CIRCUIT

In order to recover the additional energy stored in the premagnetization inductor $L_{R,A}$ during the pulse, the circuit shown in Fig. 6 is proposed [5] ($R_{R,A}$ = parasitic resistance). There, the core is premagnetized before every pulse by turning the two switches S_{R1} and S_{R2} on (cf. Fig. 7(a)) and increasing the amplitude of the magnetizing current $I_{L,\text{Mag}}$ up to the nominal value (I_{Mag}). During the premagnetization, the magnetizing inductance and the inductor $L_{R,A}$ are connected in series and build an inductive voltage divider. In order to avoid a current flowing through D_F during this period, it is important that the voltage drop across the magnetizing inductance is smaller than the forward voltage of the (series connected) freewheeling
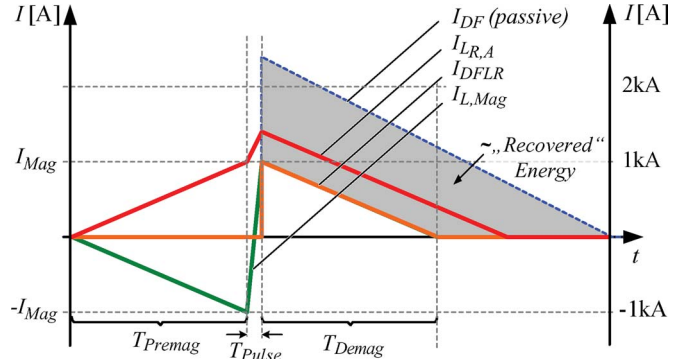

Fig. 8. Run of the current $I_{\text{DF,LV}}$ in the freewheeling diode D_F, the magnetizing current $I_{L,\text{Mag}}$, the current $I_{L,V}$ in the premagnetization inductance L_V, and—for comparison—the current in the freewheeling diode D_F for the passive reset circuit explained in Section II. The area "Recovered" Energy is proportional to the energy which is recovered by the advanced passive circuit.

diode(s) D_F. This also determines the minimal time for premagnetization (Fig. 8).

At the end of the premagnetizing period T_{Premag} one or both switches (S_{R1}/S_{R2}) are turned off, and shortly thereafter, the main switch S_M is turned on.

In case both MOSFETs are turned off, the magnetization current flows along the dashed green path via the diodes D_{R1} and D_{R2} shown in Fig. 7(b), and a small share of the energy stored in L_M and $L_{R,A}$ is fed back to the source V_{Reset} in the interlocking delay between the switching actions. During the pulse, the current $I_{L_{R,A}}$ continues to flow along the dashed green path and adds to the switch current. Thus, the total switch current at the end of the pulse is load + magnetization current + $I_{L_{R,A}}$. In analog manner, this is also true for the standard passive circuit.

In addition, the current $I_{L_{R,A}}$ increases with a larger di/dt than during the premagnetization since the voltage $V_{\text{dc}} - V_{\text{Reset}}$ lies in the positive direction across inductor $L_{R,A}$ during the pulse. Therefore, energy is transferred from the pulse source to the reset source V_{Reset}.

In case only one MOSFET is turned off, the current is freewheeling via one diode $D_{R\nu}$ and the turned on MOSFET $S_{R\nu}$ instead of flowing via the voltage source V_{Reset}. Consequently, the amplitude of the current $I_{L_{R,A}}$ is approximately constant before the main switch S_M is turned on, and this state could be used, e.g., for keeping the magnetization current constant until the pulse in case the nominal magnetization current I_{Mag} is reached before the pulse begins (e.g., due to tolerances). Another possibility is to keep the premagnetization current constant between the pulses (as with the standard passive premagnetization) if the time between the pulses is short (high repetition rate). During the pulse, turning off one MOSFET would lead to a higher di/dt than turning off both, since the voltage V_{Reset} lies across inductor $L_{R,A}$. In order to minimize the energy stored in $I_{L_{R,A}}$, it is assumed in the following that both MOSFETs are turned off during the pulse.

As soon as the main switch S_M is closed, the magnetization current starts to rise from $-I_{\text{Mag}}$ to $+I_{\text{Mag}}$. After the pulse, the energy stored in the magnetization inductance is dissipated in the freewheeling diode D_F, but the energy stored in the premagnetization inductance $L_{R,A}$ is restored to the voltage source V_{Reset}. Therefore, the losses due to the premagnetization
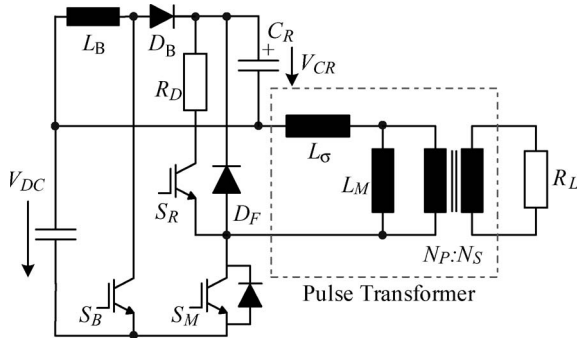
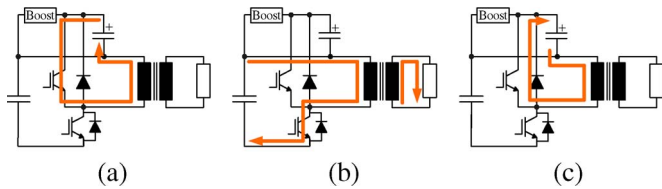Fig. 9.   Active reset circuit with energy recovery.

Fig. 10.   Current paths for the active reset circuit in the three time sections: premagnetization, pulse, and demagnetization. (a) Premagnetization. (b) Pulse. (c) Demagnetization.

are significantly lower with this circuit than with the standard premagnetization circuit (cf. Section V), and the energy, which has to be provided by the source V_{Reset}, is relatively low.

IV. ACTIVE RESET CIRCUIT

For further reducing the losses due to the premagnetization, an active reset circuit as shown, for example, in Fig. 9 could be applied [6], [8]. There, no passive components, like a premagnetization inductor, for voltage blocking/dividing or current control are utilized, and the transformer is premagnetized before each pulse.

For premagnetizing, the capacitor C_R must be charged up (e.g., by a boost converter as shown in Fig. 9) to a specific voltage level. In the considered case, 100 V($= 10\%$ of V_{dc}) is assumed. Then, the switch S_R is closed, so that a negative premagnetization current starts to flow in the primary (cf. Figs. 10(a) and 11(a)). Energy is now transferred from the capacitor C_R to the magnetizing inductance, and as soon as the nominal magnetization current I_{Mag} is reached, switch S_R is turned off. As soon as switch S_R is off, the current in the leakage inductance freewheels via the dc link capacitor and the antiparallel diode of the main switch S_M. Since the negative voltage across the leakage inductance is relatively large ($V_{L_R} = -V_{\text{dc}}$), the current in the leakage inductance decreases rapidly, and the current in the magnetizing inductance commutates to the secondary side. There, it flows via the load resistance, so that the voltage drop across the magnetizing inductance is relatively small (≈ 150 V in the considered case) and the magnetizing current decreases only slowly during this interlocking delay.

After the delay, the main switch is turned on, and the pulse is generated while the magnetizing current is ramping up from $-I_{\text{Mag}}$ to I_{Mag}. There, no additional current from a
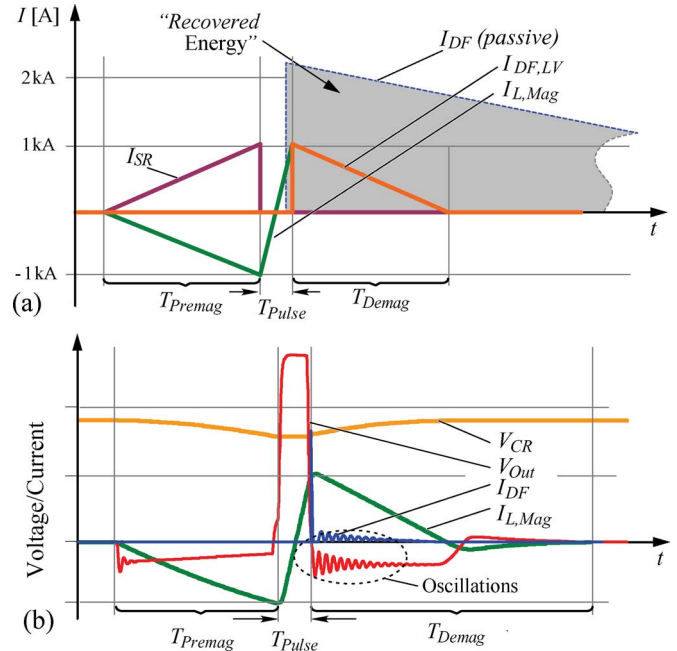

Fig. 11.   (a) Ideal run of the current $I_{\text{DF,LV}}$ in the freewheeling diode D_F, the magnetizing current $I_{L,\text{Mag}}$, the switch current I_{SR}, and—for comparison—the current I_{DF} resulting from the passive reset circuit (cf. Fig. 5). (b) Simulated waveforms for the diode current I_{DF}, the magnetizing current $I_{L,\text{Mag}}$, the output voltage V_{Out}, and the reset voltage V_{CR}.

premagnetization inductor is flowing via switch S_M as with the two passive circuits and the current stress/losses in S_M are reduced.

After the pulse, the energy stored in the magnetizing inductance L_M (and the part of the energy stored in L_σ which is not dissipated in S_M while turning off) is fed back to the reset capacitor C_R via the freewheeling diode D_F. Since the reset capacitor voltage V_{CR} is much larger than the forward voltage of the diode D_F, the losses in the diode are small, and the time for demagnetization T_{Demag} is short. Furthermore, the freewheeling diode D_F could consist of a single diode with low forward voltage($=$ low losses) since the demagnetization time is mainly defined by V_{CR}.

Due to the losses in the diode D_F, the switch S_R, the damping resistor R_R, and the transformer, the voltage across C_R is a bit smaller after the energy recovery than before the pulse. These losses/voltage drop can be compensated, e.g., by a boost converter, so that a symmetric flux swing ΔB_2 around zero is generated (cf. Fig. 2).

Another possibility is to use a slightly asymmetric flux swing for compensating the losses/voltage drop. In this case, the negative premagnetization amplitude $B_{\text{Reset}}(S_2)$ (cf. Fig. 2) is made a bit smaller than the positive one B_{Max}. Consequently, also the negative magnetizing current amplitude is smaller than the positive one, and for premagnetizing the transformer, less energy is required than is stored in the magnetization inductance after the pulse. Therefore, more energy is fed back to C_R than is used for premagnetizing, which compensates for the losses. This effect is self-stabilizing, i.e., the flux swing automatically shifts to a position, where the energy stored after the pulse is equal to the energy required for premagnetizing plus the losses.

One important fact to notice is that, during the pre-magnetization, a negative voltage has to be applied to the primary/magnetizing inductance for increasing the amplitude of the magnetizing current. This voltage is also reflected to the secondary/load. In case of a klystron load, for example, this negative voltage does not cause any current flow if it is below a limit depending on the klystron specifications. The larger this value could be, the faster the pre- and demagnetization will take place.

This effect is also true for the two described passive reset circuits, but there, the negative voltage (defined by the forward voltage of the (series connected) freewheeling diodes) usually is smaller. This, however, also results in a longer pre-/demagnetization time.

In case the negative voltage is too large, a smaller voltage V_{CR} could be used. This results in a longer pre-/demagnetization time and increases the losses.

During the pre- and demagnetization, the magnetizing inductance L_M is connected in parallel to the parasitic capacitances of the transformer [9] and in series to the reset capacitor C_R and the leakage inductance L_σ. Due to the steplike excitation by switching S_R, oscillations occur. By inserting the damping resistor R_D, the oscillations can be significantly damped as could be seen in the simulated waveforms shown in Fig. 11(b). There, also the run of the capacitor voltage V_{CR}, the load voltage V_{Out}, and the current I_{DF} is shown. The waveform of I_{DF} shows a very short but high positive peak when S_M is turned off, which is caused by the current flowing through the leakage inductance L_σ, which has been neglected so far. This current decreases rapidly since it flows via the load R_L and causes only small losses.

The ringing shown in Fig. 11(b) are more damped in reality due to HF losses in the transformer, slower switches, and interconnection resistances which have not been considered in the simulation.

V. COMPARISON

With all three circuits presented in the previous sections, a premagnetization of the transformer is basically possible. In order to compare the circuits, the losses and the component stresses have been calculated for a pulse modulator design shown in Fig. 1 operating with the specifications given in Table I. The resulting losses in the components are summarized in Table II.

In the case of the passive circuit, the 1.45-kW total loss result is mainly caused by the high losses in the freewheeling diode D_F. A share of 250 W of the total losses is caused in the parasitic resistance R_R of the inductor/transformer winding. The calculated losses for the passive circuit correspond very well to measured losses, which are approximately 13% smaller due to component tolerances. Further measurement results will be presented in a future paper.

With the advanced passive circuit, the losses in the diode D_F can be almost reduced by a factor of five, since the energy in the premagnetization inductor $L_{R,A}$ is recovered. In the auxiliary circuit for controlling the current in the magnetizing inductance L_M and in the inductor $L_{R,A}$, however, additional 150 W of

TABLE II
CALCULATED LOSSES OF THE RESET CIRCUITS FOR THE SPECIFICATIONS GIVEN IN TABLE I. THE PARAMETERS FOR THE STANDARD PASSIVE RESET CIRCUIT ARE $L_R = 5.4$ mH$/R_R = 0.1\ \Omega/D_F = 10$ V. FOR THE ADVANCED PASSIVE ONE, THEY ARE $L_{R,A} = 13.5\ \mu$H$/R_{R,A} = 250\ \mu\Omega/D_F = 10V/R_{\mathrm{DS,on}} = 2\ \mathrm{m}\Omega/V_{\mathrm{DF},DR\nu} = 1$V, AND FOR THE ACTIVE RESET ONE, THEY ARE $R_D = 30\ \mathrm{m}\Omega/D_F = 2.5$ V$/V_{\mathrm{IGBT}} = 2.5$ V

Passive	Advanced	Active
Freewheeling Diode D_F (per pulse/@200Hz)		
5.95J	1.25J	0.283J
1.2kW	250W	56.6W
Resistor (per pulse/@200Hz)		
-	0.042J	0.50J
250W	8.4W	100W
Auxiliary Circuit (per pulse/@200Hz)		
–	$D_{R1,2}/D_{F,LR}$: 0.75J/150W $S_{R1,2}$: 0.34J/ 68W	IGBT S_R: 0.064J 12.8W
Total Losses (per pulse/@200Hz)		
7.25J	2.38J	0.85J
1.45kW	476.4W	169.4W

TABLE III
PROS AND CONS OF THE RESET CIRCUIT TOPOLOGIES.
(* FOR MINIMAL LOSSES)

	Passive	Advanced	Active
Complexity	Simple/Robust	high	medium
Components	Voltage Source low I / low V	MOSFET/Diode high I / low V	IGBT high I / high V
	Inductor low I / high V	Diode $D_{F,LV}$ high I / high V	Capacitor high I / med. V
Third Winding	yes*	no	no
Forward V_{DF}	high (10V)	high (10V)	low (2V)
Volume	high	high	medium

losses are caused in the diodes and 68 W in the MOSFETs. Therefore, only a reduction of approximately a factor of three is achieved for the total losses.

With the active reset circuit, the losses in diode D_F can be further reduced to 56.6 W. In the damping resistor R_D, however, significant losses of 100 W are generated, resulting in an improvement of approximately a factor of 8.5 regarding the overall losses compared to the standard passive circuit.

Besides the losses, also the amount of components and their stress is important for comparing the circuits. In Table III, different advantages and disadvantages of the circuits are summarized. There, it could be seen that the complexity of the passive circuit is low, but a third transformer winding and a high voltage inductor (> 20 kV) are required for achieving the values shown in Table II. Basically, an operation without a third winding is possible but this does not result in minimal losses [4]. Furthermore, the forward voltage of the freewheeling diode must be high (short time for demagnetization/high repetition frequency), which leads in total in a relatively large volume for the reset circuit, which is also caused by the additional cooling effort.

With the advanced passive circuit, the complexity increases, but no third winding is required, and the losses/cooling effort are lower. The forward voltage of diode D_F and the current

rating of the switches $S_{V1,2}(\sim 75 - 100 \text{ V}/ > 1\text{-kA peak})$, however, must be high. Due to the required inductor and the auxiliary circuit, the system volume is again high.

A lower system volume could be achieved with the active circuit where mainly the capacitor C_R (e.g., 750 μF/100 V/1 kA in the considered case) determines the size. Also, the complexity of the circuit is lower than with the advanced passive one. However, the switch S_R must have a high voltage and current rating (1700 V / >1 kA peak) as well as the single freewheeling diode D_F. Additionally, the main switch S_M must have an antiparallel diode, so that the current in the leakage inductance could flow via the dc link capacitor and the freewheeling diode after switch S_R has been turned off and before switch S_M is turned on.

Remark on costs: For the two passive circuits, a high forward voltage of the freewheeling diode is required (= series connection of three diodes in the considered case), and for the active circuit, a low forward voltage is sufficient (= 1 diode). For the active circuit, however, a high voltage/current switch (here, SKM400GAL176D from Semikron are used) is required, which significantly increases costs. On the other hand, the cooling costs for the passive circuits are higher than those for the active one. In total, the initial costs of the three systems are comparable, but the running costs for the active circuit are significantly lower, which makes this system very attractive also from a cost point of view.

VI. CONCLUSION

In this paper, three different circuits for generating a negative premagnetization of pulse transformers are presented and compared: the standard passive circuit, an advanced passive circuit, and an active circuit. The well-known standard circuit has only the advantage of low complexity/robustness but causes relatively high losses and significantly influences the system efficiency. Therefore, a new advanced passive circuit which enables a loss reduction by a factor of three based on a pulse-by-pulse premagnetization is proposed. In the advanced passive reset circuit, mainly low-voltage power semiconductors are required. However, the system complexity is higher than with the standard passive one.

For reducing the losses further, an active reset circuit that leads to a loss reduction by a factor of 6.5 is presented. This circuit is also based on a pulse-by-pulse premagnetization, where most of the energy stored in the magnetizing inductance is recovered and stored in an additional capacitor. There, it is important to note that, during the premagnetization, the voltage of the reset capacitor is reflected to the output, so that a negative output voltage ($\sim$2.5%–20% depending on the design) appears. In case this could not be tolerated by the load, one of the two presented passive circuits must be used.

REFERENCES

[1] N. G. Glasoe and J. V. Lebacqz, *Pulse Generators*, ser. MIT Radiation Laboratory Series, vol. 5. New York: McGraw-Hill, 1948.
[2] P. W. Smith, *Transient Electronics, Pulsed Circuit Technology*. West Sussex, U.K.: Wiley, 2002.
[3] S. Roche, *Solid State Pulsed Power Systems*, Marsannay la cote, France: Physique Industrie. [Online]. Available: www.physiqueindustrie.com
[4] D. Bortis, J. Biela, and J. W. Kolar, "Optimal design of a DC reset circuit for pulse transformers," in *Proc. APEC*, Anaheim, CA, Feb. 25–Mar. 1, 2007, pp. 1171–1177.
[5] D. Bortis, J. Biela, and J. W. Kolar, "Patent," Patent Application Filed as Swiss Patent 00 994/07, Jun. 21, 2007.
[6] H. Kirbie, "Unified power architecture," U.S. Patent 6 529 387, Mar. 4, 2003.
[7] D. A. Smith, "Zero voltage switching power converter," U.S. Patent 5 173 846, Dec. 22, 1992.
[8] H. Kirbie, "Unified Power Architecture With Dynamic Reset," U.S. Patent 6 466 455, Oct. 15, 2002.
[9] J. Biela, D. Bortis, and J. W. Kolar, "Analytical modeling of pulse transformers for power modulators," in *Proc. Int. Power Modulator Conf.*, Washington, DC, 2006, pp. 135–140.

Juergen Biela (S'04–M'07) studied electrical engineering at the FAU Erlangen, Germany, receiving the Diploma degree with honors in October 2000. During his studies, he dealt in particular with resonant dc-link inverters at Strathclyde University, U.K., and the active control of series-connected IGCTs at the Technical University of Munich, Germany. Since July 2002, he has been working toward the Ph.D. degree at the PES, ETH Zurich, Switzerland, where, since January 2006, he has also been a Postdoctoral Researcher.

After he received the Diploma degree, he worked on inverters with very high switching frequencies, SiC components, and EMC in the Research Department of A&D Siemens, Germany.

Dominik Bortis (S'06) was born in Fiesch, Switzerland, on December 29, 1980. He received the B.S. degree in electrical engineering from the Eidgenoessische Technische Hochschule (ETH) Zurich, Zurich, Switzerland, where he majored in communication technology and automatic control engineering, the M.Sc. degree in May 2005 from ETH Zurich, and he has been working toward the Ph.D. degree at the Power Electronic Systems Laboratory, ETH Zurich, since June 2005.

In his diploma thesis, he was with the company Levitronix, where he designed and realized a galvanic isolation system for analog signals.

Johann W. Kolar (S'89–M'89–SM'04) received the B.S. degree in industrial electronics and the Ph.D. degree (*summa cum laude*) from Vienna University of Technology, Vienna, Austria.

From 1984 to 2001, he was with Vienna University of Technology, where he was teaching and working in research in close collaboration with industry. He has proposed numerous novel converter topologies, e.g., the VIENNA rectifier and the three-phase ac–ac sparse matrix converter concept. He has published over 200 scientific papers in international journals and conference proceedings and is the holder of more than 50 patents. He has been a Professor and the Head of the Power Electronic Systems Laboratory, Eidgenoessische Technische Hochschule Zurich, since February 1, 2001.